Available online at www.sciencedirect.com
ScienceDirect
C. R. Physique 8 (2007) 986–998
COMPTES RENDUS PHYSIQUE
http://france.elsevier.com/direct/COMREN/

The mystery of the Higgs particle/Le mystère de la particule de Higgs

The Higgs boson of the Standard Model

Michel Davier

Laboratoire de l'Accélérateur Linéaire, IN2P3/CNRS, université Paris-sud 11, 91898 Orsay cedex, France

Available online 23 May 2007

Abstract

An introduction is made to the key concepts of gauge invariance and spontaneous symmetry breaking which are the foundations of the Standard Model of particle physics. A new scalar field corresponding to a spin-0 particle, the Higgs boson, is a necessary consequence of this model. Properties of the Higgs boson are constrained; however, its mass is not. Searches using LEP have been both unique, intense, and also efficient: the Standard Model Higgs boson must be heavier than 114 GeV/c^2. A hint of a signal was obtained at 115 GeV/c^2, but will have to be confirmed (or falsified) by forthcoming experiments at the Tevatron and LHC. ***To cite this article: M. Davier, C. R. Physique 8 (2007).***

Résumé

Le boson de Higgs dans le Modèle Standard. Les concepts importants d'invariance de jauge et de la brisure spontanée de symétrie qui sont à la base du Modèle Standard de physique des particules sont exposés. Une conséquence du modèle est l'existence d'un nouveau champ scalaire matérialisé par une particule de spin 0, le boson de Higgs. Le Modèle Standard fixe bien les propriétés du boson de Higgs, sauf sa masse. Les recherches effectuées au LEP ont été à la fois uniques, intenses, mais aussi efficaces : la masse du boson de Higgs est au delà de 114 GeV/c^2. Une indication de signal a été obtenue à 115 GeV/c^2, mais doit être confirmée (ou infirmée) par les expériences en cours au Tevatron ou à venir au LHC. ***Pour citer cet article : M. Davier, C. R. Physique 8 (2007).***

Keywords: Gauge invariance; Spontaneous symmetry breaking; Higgs particle; Radiative corrections

Mots-clés : Invariance de jauge ; Brisure spontanée de symétrie ; Boson de Higgs ; Corrections radiatives

1. The electroweak gauge theory

1.1. Gauge symmetries: the example of electromagnetism

Certainly one of the most spectacular advances in physics in the second part of the 20th century has been the elegant and productive description of electromagnetic, weak and strong interactions by gauge field theories. In these theories the form of the interaction is generated by postulating an invariance with respect to gauge transformations. This well-known property of electromagnetism has been successfully transferred to the weak and strong interactions, opening a new era in the understanding of the fundamental interactions.

E-mail address: davier@lal.in2p3.fr.

1631-0705/$ – see front matter
doi:10.1016/j.crhy.2006.12.002

Nomenclature

QED	Quantum Electrodynamics	*SLC*	Stanford Linear Collider, Stanford University, California, USA
QCD	Quantum Chromodynamics	*FNAL*	Fermi National Laboratory, Batavia, Illinois, USA
CERN	Centre Européen de Recherches Nucléaires, Genève	*ALEPH, DELPHI, L3, OPAL*	the four LEP detectors, CERN, Genève
LEP	Large Electron Positron Project, CERN, Genève		
LHC	Large Hadron Collider, CERN, Genève		

A simple manifestation of gauge invariance is seen in electrostatics where the electric field, and hence the electrostatic force, depend only on the *difference* of potential. More generally in electromagnetism, the vector potential $A^\mu(x)$, which is related to the electromagnetic field strength by $F^{\mu\nu} = \partial^\mu A^\nu - \partial^\nu A^\mu$, is invariant under gauge transformations,

$$A^\mu(x) \to A^\mu(x) + \partial^\mu \Lambda(x) \tag{1}$$

where $\Lambda(x)$ is an arbitrary function of space and time.

Gauge invariance is also familiar from the quantum mechanics description of a charged particle interacting with an electromagnetic field. This principle is carried over to the relativistic quantum case by requiring that all derivatives ∂_μ be replaced by *covariant derivatives* $D_\mu = \partial_\mu - \mathrm{i}qA_\mu$. As a consequence, all charged particles couple exactly in the same way to the electromagnetic field, i.e. the coupling is universal. Then, charged fields and their covariant derivatives have identical local transformations,

$$\psi(x) \to U(x)\psi(x), \quad D_\mu\psi(x) \to U(x)D_\mu\psi(x), \quad U(x) = \mathrm{e}^{\mathrm{i}q\Lambda(x)} \tag{2}$$

The $U(x)$ transformations in Eq. (2), form a $U(1)$ group, which is Abelian, since it does not matter in which order we apply successive transformations. Thus, quantum electrodynamics (QED) is described by a gauge theory where the gauge transformations belong to the $U(1)$ group. Gauge invariance requires the photon to be massless, as a term $m^2 A_\mu A^\mu$ in the Lagrangian would not be invariant. In fact the latter depends only on field configurations corresponding the only two helicity states ± 1 of a spin-1 massless particle (transverse polarizations).

The beauty about the property of gauge invariance of electromagnetism is that it can be reversed: postulating gauge invariance leads to the correct form of the electromagnetic interaction. In other words, the dynamical content of the theory follows directly from the invariance properties. The agreement of ever-more precise measurements with detailed calculations within QED is very impressive.

1.2. The electroweak unification

It was natural to extend the successful gauge invariance principle to the weak interaction [1]. However, important differences with QED prevented this for some time. First of all, weak processes imply a transition between different fermion fields: from μ to ν_μ and e to ν_e in muon decay, from neutron to proton (or d to u quarks) in β decays of nuclei, whereas the electromagnetic current connects identical charged fermions. Then, weak interactions are not invariant under space inversion, unlike electromagnetic interactions. This parity violation is even maximal, leading to a description of the weak current in terms of equal-magnitude vector and axialvector currents (the so-called $V - A$ current). In other words, only left-handed fields are involved. Chirality (left-handed and right-handed states) of a fermion corresponds, at high-energy, to its helicity state. An electron field can be decomposed then as $e = e_L + e_R$. Electromagnetism treats these two components on an equal footing, preserving symmetry under parity. Indeed the gauge coupling of electrons to photons reads $\bar{e}\gamma^\mu A_\mu e = \bar{e}_L\gamma^\mu A_\mu e_L + \bar{e}_R\gamma^\mu A_\mu e_R$, where γ^μ are Dirac matrices which can be thought of as a relativistic generalisation of the Pauli spin matrices. In contrast, the charged current to which one would like to associate a charged gauge boson, $W^\pm$, is of the form, $\bar{e}_L\gamma^\mu W_\mu^+ \nu_{e(L)}$. To make this resemble the electromagnetic current, one can write it as $\bar{E}_L\gamma^\mu W_\mu^+ \tau^+ E_L$. The entity $E_L = \binom{\nu_e}{e_L}$ should be considered as a doublet (one speaks of an isospin doublet) and $\tau^\pm$ are the raising and lowering Pauli matrices.

The smallest group of gauge transformations acting on the doublet E_L (and n, p) generalising Eq. (2), is $SU(2)_L$, the non-Abelian isospin group, which besides $\tau^{\pm}$ has also 'a neutral' generator τ^3. There will therefore be 3 gauge fields: $W^{\pm}_{\mu}, W^3_{\mu}$. $SU(2)_L$ symmetry predicts the coupling of W^3: $\bar{E}_L\gamma_\mu W^3_\mu \tau^3 E_L = \bar{\nu}_e\gamma_\mu W^3_\mu \nu_e - \bar{e}_L\gamma_\mu W^3_\mu e_L$. This neutral current cannot correspond to the electromagnetic current. On the one hand, it involves neutrinos which are uncharged. On the other hand, it only includes the left-handed part of the electromagnetic current. So something more involved is needed. To fully reconstruct the electromagnetic current from the neutral isospin current, one must postulate the existence of at least another neutral current. In the standard model this is introduced via a $U(1)_Y$ neutral current, associated with a weak hypercharge Y and a gauge field B_μ. The latter couples to both the left-handed doublet and right-handed (e.g. e_R) isospin singlet. The photon and the Z then appear as a superposition of the fields B_μ and W^3_μ.

Quarks also form doublets Q under $SU(2)$, such as (u, d), which determine the structure of the weak current between them. However, quarks are bound into hadrons by the strong force, which is also described by a gauge theory called quantum chromodynamics (QCD). Each quark carries a strong 'charge', called 'colour', belonging to a set of three colours. The messenger of the colour force is the gluon. The gauge group here is $SU(3)$, with 8 types of gluons, corresponding to the 8 generators of the fundamental representation of $SU(3)$. (e, ν_e, u, d) form the first family of matter particles of the SM model, among the 3 which have been discovered.

Coming back to the weak and electromagnetic interactions, let us call g, g' the gauge coupling constants of the fundamental gauge interactions, generated by invariance through $SU(2)_L$ and $U(1)_Y$ groups. The gauge transformations and the covariant derivative generalizing Eq. (2) are then

$$\psi(x) \to \mathrm{e}^{\mathrm{i}\theta_2^j(x)\frac{\tau^j}{2}}\mathrm{e}^{\mathrm{i}\theta_1(x)Y}\psi(x), \quad D_\mu = \partial_\mu - \mathrm{i}g\frac{\tau^i}{2}W^i_\mu - \mathrm{i}g'YB_\mu \tag{3}$$

The covariant derivatives completely specify the interactions of all known fermions and gauge bosons and encode the universality of the gauge couplings via the matter Lagrangian

$$L_{\text{matter}} = \sum_{j=Q,u_R,d_R,L,e_R,\nu_R} \overline{\psi}_j \mathrm{i}\gamma^\mu D_\mu \psi_j \tag{4}$$

In non-Abelian gauge theories, as a consequence of the gauge transformations, the gauge fields are self-interacting: not only do the matter fields carry charge, but also the gauge fields.

1.3. Gauge boson masses: from the Higgs mechanism to the Higgs boson

A major obstacle to the electroweak theory so far presented is the fact that the weak force is experimentally found to be short ranged, leading to massive $W^{\pm}$ and Z bosons. This is inconsistent with gauge invariance. The problem was solved by borrowing and adapting an idea successfully used for several solid-state physics phenomena. In such systems, the Hamiltonian is invariant under a symmetry while the *ground state* of the system breaks this symmetry. Such is the case with a ferromagnet below the Curie temperature. In this case, rotational symmetry is broken by the ground state (all spins of the atoms are aligned in the same direction) despite the fact that the dynamics (the Heisenberg spin–spin Hamiltonian) does not select any preferred direction. This spontaneous symmetry breaking is also at work in superconductivity where, with the Meissner effect, the fact that the magnetic field enters the solid over a very short range could be associated with a massive photon.

One usually thinks about (and most often defines) the vacuum as a state where all fields have zero expectation value. However it may happen, like the situation depicted in Fig. 1, that the state with zero energy is not the most stable. The system will choose stability or minimum energy (bottom of the well) rather than the state with maximum symmetry (top of the mountain). Such potentials are provided by scalar fields, with a potential of the form $V = \lambda(|\phi|^2 - v^2/2)^2$ ($\lambda > 0$), where v is the vacuum expectation value (v.e.v.) of the scalar field $\langle 0|\phi|0\rangle = v/\sqrt{2}$. This scale is at the origin of the mass of the gauge bosons and also, as we shall see, the fermions.

To see how this works, it is simplest to take QED as an example [2] to illustrate how a mass for the photon can be introduced in a *gauge invariant* way. One needs to introduce a charged scalar field ϕ. The latter can be represented by a complex field $\phi = (\phi_1 + \mathrm{i}\phi_2)/\sqrt{2}$. For our purposes it is best to rewrite it in polar coordinates as $\phi = (h + v)\mathrm{e}^{\mathrm{i}\theta/v}/\sqrt{2}$, where both h and θ have zero v.e.v. While θ characterises the rotational symmetry of the potential, h describes fluctuations around the potential minimum. The interaction of this scalar field with the electromagnetic field is described by

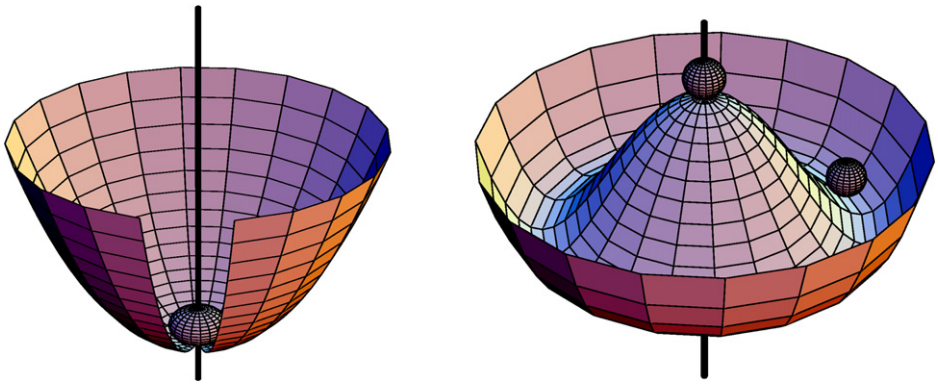

Fig. 1. Two-dimensional visualization of scalar potentials. The left plot shows a symmetric potential, under rotation around the vertical axis, with a stable minimum where the ball is resting. In this situation $\langle 0|\phi|0\rangle = 0$. The right figure, resembling a Mexican hat, illustrates spontaneous symmetry breaking. The symmetric configuration at the top of the hat is unstable. The system will pick up *any* stable configuration along the brim with $\langle 0|\phi|0\rangle \neq 0$. The Goldstone vibration modes are along this azimuthal direction whereas the radial component is the Higgs field.

a fully gauge invariant Lagrangian constructed through the use of the covariant derivative, Eq. (2). Upon expansion of this Lagrangian one finds

$$L = -\frac{1}{4}F_{\mu\nu}F^{\mu\nu} + \frac{1}{2}v^2\left(eA_\mu + \frac{1}{v}\partial_\mu\theta\right)^2 + \frac{1}{2}\partial_\mu h\partial^\mu h - \frac{\lambda}{4}\left(h^2+2vh\right)^2 + \frac{1}{2}\left(eA_\mu + \frac{1}{v}\partial_\mu\theta\right)^2\left(h^2+2vh\right) \quad (5)$$

One sees clearly that the gauge field has acquired a mass, $m_\gamma = ev$ (second term in Eq. (5): $+e^2v^2A_\mu A^\mu/2$). Because of gauge invariance, we can always make a (local) phase transformation on the field $\phi = (h+v)\mathrm{e}^{\mathrm{i}\theta/v}/\sqrt{2}$ such that the 'phase' θ/v is set to zero. This gauge where $\theta \to 0$ in Eq. (5) is the *unitary gauge* where only the *physical states* h, A_μ are left. Counting the number of degrees of freedom before and after symmetry breaking, we find the same number, of course. Before, one had two scalars and one massless spin-1 which has only two (transverse) states of polarisation, therefore four degrees of freedom. After symmetry breaking, one of the scalars, θ, transmutes into the longitudinal polarisation of the 'heavy photon'. In fact it would be more appropriate to say that the gauge symmetry is hidden, once we choose a particular gauge, since the gauge symmetry is present in the dynamics. The θ field corresponds, as seen in Eq. (5), to a massless pseudo-scalar particle, called a Goldstone boson, h is the Higgs scalar field whose mass is given by $\sqrt{2\lambda v^2}$. There is also a coupling hAA which is proportional to the mass of the gauge boson, as well as trilinear $3h$ and quadrilinear $4h$ couplings.

A very similar approach is applied to the weak interaction under $SU(2)_L \times U(1)$. Since we need three massive gauge bosons, the three longitudinal states will be provided by three Goldstone bosons. This is most simply and economically provided by a Higgs doublet, Φ, with quantum numbers such that the vacuum is left invariant under electromagnetic gauge transformations, so that the photon remains massless:

$$\Phi = \begin{pmatrix} 0 \\ \frac{1}{\sqrt{2}}(v+H) \end{pmatrix}\mathrm{e}^{\mathrm{i}\omega^j\frac{\tau^j}{2v}}, \quad L_{\text{Higgs}} = (D^\mu\Phi)^\dagger(D_\mu\Phi) - V(\Phi^\dagger\Phi) \quad (6)$$

with

$$V(\Phi^\dagger\Phi) = \lambda\left(\Phi^\dagger\Phi - \frac{v^2}{2}\right)^2 \quad (7)$$

where H is the physical Higgs field of the electroweak theory, $\omega^{1,2,3}$ the Goldstone boson fields and v the vacuum expectation value. After symmetry breaking, the $W^\pm$ and Z^0 bosons have acquired mass and there remains a scalar Higgs boson which should be experimentally found.

1.4. Fermion masses and Higgs boson properties

We already stressed the fact that QED treated both electron chiralities on the same footing, in particular e_L and e_R have the same electric charge. Therefore the electron mass term $m_e(\bar{e}_R e_L + \bar{e}_L e_R)$ is gauge invariant in QED.

Since the SM has no left and right-handed multiplets with identical $SU(2)$ and $U(1)_Y$ charges, a fermion mass term introduced by hand would break the gauge symmetry. However, mass terms are possible via the Higgs mechanism. Let us consider the masses for the charged leptons, but the same approach applies to the quarks as well. The left-handed doublet L, the right-handed singlet l_R and the Higgs field Φ combine so that they form a neutral symmetric object under $SU(2) \times U(1)$, with so-called Yukawa couplings y_l. The masses then appear as

$$-L_m^l = \sum_{i=e,\mu,\tau} y_l^i \left(\bar{L}_i \Phi l_{R,i} + \bar{l}_{R,i} \Phi^\dagger L_i\right) \longrightarrow \sum_{i=e,\mu,\tau} \frac{y_l^i v}{\sqrt{2}} \left(1 + \frac{H}{v}\right) \bar{l}_i l_i, \quad \frac{y_l^i v}{\sqrt{2}} = m_l^i \tag{8}$$

An important consequence of this mass generation scheme is that it determines the couplings of the Higgs to fermions which are found to be proportional to the fermion mass. In other words, the introduction of mass terms through the Higgs symmetry-breaking mechanism completely fixes the Higgs phenomenology, i.e. the way the Higgs boson can be produced and the way it will decay, both aspects being accessible in experiments. Because in the quark sector one is generating masses for both the up and down quark, one also induces mixing between the three-families in the charged current [3] (but not in the neutral currents [4]). This is also the source of CP-violation in the model. It is important to stress that although masses and mixing are introduced in a gauge invariant way, one nonetheless needs to introduce a large number of ad-hoc Yukawa couplings, contrary to the gauge boson masses that are expressed through the universal gauge coupling.

2. Precision tests of the Standard Model

2.1. Couplings and mass relations at lowest order

Let us summarize at this point the main predictions of the electroweak Standard Model which can be experimentally tested:

- The Higgs Lagrangian generates mass terms for the charged $W^\pm$ and for Z fields. W_μ^3 and B_μ combine to give the massless photon and the Z,

$$Z_\mu = \cos\theta_W W_\mu^3 - \sin\theta_W B_\mu = \frac{1}{\sqrt{g^2 + g'^2}} \left(g W_\mu^3 - g' B_\mu\right)$$
$$A_\mu = \sin\theta_W W_\mu^3 + \cos\theta_W B_\mu \tag{9}$$

  These relations define the weak mixing angle θ_W, which satisfies the 'unification' relation:

$$g \cos\theta_W = g' \sin\theta_W = e \tag{10}$$

- The W and Z masses are given by

$$M_W = \frac{gv}{2} \quad \text{and} \quad M_Z = \sqrt{g^2 + g'^2}\,\frac{v}{2} = \frac{M_W}{\cos\theta_W} \tag{11}$$

  The relation $\rho = M_W^2 / M_Z^2 \cos^2\theta_W = 1$ is a consequence of the breaking the electroweak symmetry by a scalar doublet Higgs field. Other Higgs isospin configurations would lead to $\rho \neq 1$.
- The mass terms for the W and Z are directly related to HWW and HZZ couplings, of strength $2M_W^2/v$ and $2M_Z^2/v$, respectively. This coupling of a single scalar to two gauge bosons requires the existence of a v.e.v. for the Higgs doublet field. Normally, gauge bosons couple to pairs of scalars only.
- The Higgs boson mass is given by $M_H^2 = 2\lambda v^2$. Since the quartic coupling λ is a free parameter, there is no intrinsic prediction for M_H within the Standard Model.
- The same Higgs mechanism is responsible for the mass of the fermions. The coupling of the Higgs being proportional to the mass of the fermion, an intermediate mass Higgs, $M_H < 2M_W$, would decay predominantly to the heaviest kinematically-accessible quarks, i.e. b-quarks. This strong preference for heavy quarks is a clear experimental signature of Higgs boson decays.

It is important to stress that the model gives a very nice unified description of the weak and electromagnetic interactions. However the model does not fully unify these interactions, since we still have *two* (independent) gauge couplings g, g'. Viewed another way the model does not *predict* $\sin\theta_W$. Nonetheless the gauge principle automatically leads to the universality of the gauge coupling. Most importantly, the neutral interaction Lagrangian derived from Eq. (4), summarises the main properties and parameters of Z physics:

$$L^{NC}_{\text{matter}} = e\sum_i Q_i \overline{\psi}_i \gamma^\mu \psi_i A_\mu + \frac{e}{2s_W c_W}\sum_i \overline{\psi}_i \gamma^\mu (v_i - a_i\gamma_5)\psi_i Z_\mu \tag{12}$$

with the vector and axial-vector Z couplings to fermion-antifermion i pairs given by ($s_W = \sin\theta_W$, $c_W = \cos\theta_W$)

$$v_i = I_3(i) - 2Q_i s^2_W, \qquad a_i = I_3(i) \tag{13}$$

2.2. Electroweak radiative corrections

Leaving aside fermion masses, the fermion and gauge field Lagrangians considered above are completely determined in terms of just four free parameters. These can be taken as the gauge couplings g, g', the Higgs v.e.v. v, and the quartic Higgs coupling λ. In particular the first three parameters alone allow one to determine all the properties of the gauge weak bosons (masses and self-couplings) as well as their interaction with matter. This is the power and beauty of gauge invariance that, with a limited number of parameters, one can describe a large number of processes and observables. For example at the Z peak, at LEP and SLC, the mixing angle $s_W = \sin\theta_W$ has been extracted with high precision from the ratio of a number of cross-sections which measure the coupling g^f_V/g^f_A. The final LEP measurement of s^2_W from leptonic observables [5] gives an average value

$$s^2_l = 0.23153 \pm 0.00016 \text{ (i.e. 0.07\% precision)} \tag{14}$$

Since s_W also describes the ratio M^2_W/M^2_Z, it can be also extracted from a combination of entirely different measurements (M_Z from the Z resonance and above the W^+W^- threshold from W decays).

The latest data [5] give $M_Z = (91.1875 \pm 0.0021)$ GeV/c^2 ($\Delta M_Z/M_Z \sim 2\times 10^{-5}$) and $M_W = (80.410 \pm 0.032)$ GeV/c^2 ($\Delta M_W/M_W \sim 5\times 10^{-4}$), leading to

$$s^2_M = 0.22141 \pm 0.00062 \text{ (i.e. 0.3\% precision)} \tag{15}$$

The two experimental determination of s^2_W, which should be identical in the Standard Model, in fact are found to differ by 14 standard deviations! This reminds us of a similar situation encountered for electromagnetic quantities, such as the electron magnetic moment predicted by Dirac to be exactly equal to one Bohr magneton, but experimentally observed to be slightly (but unambiguously) different. The small deviation (at the 10^{-3} level) is actually due to the contribution of higher-order terms in the electromagnetic perturbative expansion. Once these contributions are included in the prediction , which is done these days up to the 4th order in the electromagnetic coupling (the fine structure constant α), in order to match the accuracy of the measurement, the agreement between theory and experiment becomes excellent [6], even limited by an independent knowledge of α at this level of precision.

Thus one should consider the effect of higher-order contributions (generally called 'radiative corrections') in the electroweak theory. Such calculations are possible in a consistent way because of the gauge invariance of the theory [7]. Some prominent contributions, illustrated by the corresponding Feynman diagrams (a way to visualise the physical process, but also an important tool in the actual calculations), are given in Fig. 2. It can be seen that many of these corrections originating from quantum fluctuations of the vacuum (called vacuum polarization in analogy to macroscopic polarization in a dielectric material), as evidenced by the creation/absorption of a pair of particles (so-called 'loops') from the propagating photon or vector boson exchanged in the interaction. These calculations are not straightforward and generally lead to divergent results. This problem is cured by a redefinition of the fundamental constants of the theory, as it is well known in quantum electrodynamics where the electric charge is 'renormalized' when radiative corrections are taken into account.

Since the precise prediction of observables in the Standard Model will now depend on radiative corrections, it is easy to see that the comparison with experiment will actually be sensitive to the effect of particle loops which depends on the mass of these particles. The exciting part of this exercise is that it gives access to the mass of new, as yet

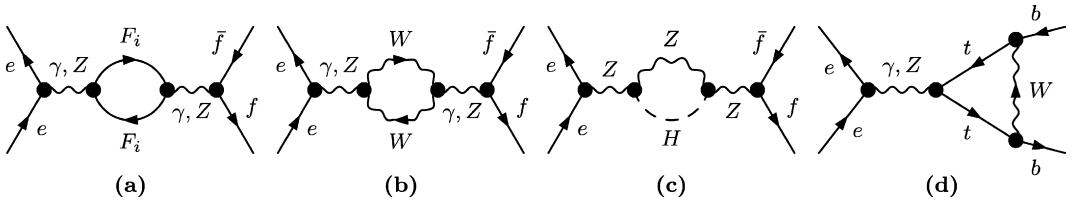

Fig. 2. Some of the processes representing the quantum loop corrections to $e^+e^- \to f\bar{f}$, expressed as Feynman diagrams. The first three diagrams involve vacuum polarization. Diagram (d) is a vertex correction with virtual top quarks which contributes to $b\bar{b}$ production.

undiscovered, particles which are too heavy to be directly produced in experiments, but can be 'felt' through vacuum polarization.

The most precisely measured quantities of the Standard Model are the QED fine structure constant $\alpha = e^2/4\pi$, the Z mass M_Z, and the Fermi constant G_μ derived from muon decay (which at lowest-order is $G_\mu/\sqrt{2} = g^2/8M_W^2$). Choosing these parameters as input to the theory calculations, in lieu of the three fundamental parameters g, g' and v of the original Lagrangian, one finds that

$$
\begin{aligned}
&s_M^2 \simeq s_Z^2\left(1 + \frac{c_W^2}{c_W^2 - s_W^2}\Delta\hat{r}\right); \quad \Delta\hat{r} \simeq -\frac{c_W^2}{s_W^2}\varepsilon_1 + \frac{c_W^2 - s_W^2}{s_W^2}\varepsilon_2 + 2\varepsilon_3 \\
&s_l^2 \simeq s_Z^2\left(1 + \frac{c_W^2}{c_W^2 - s_W^2}\Delta\kappa\right); \quad \Delta\kappa = \simeq \left(-\varepsilon_1 + \frac{\varepsilon_3}{c_W^2}\right) \\
&s_Z^2 = \frac{1}{2}\left(1 - \sqrt{1 - \frac{4\pi\alpha(M_Z^2)}{\sqrt{2}G_\mu M_Z^2}}\right); \quad \alpha\left(M_Z^2\right) = \frac{\alpha}{1 - \Delta\alpha(M_Z^2)}
\end{aligned}
\tag{16}
$$

The most important corrections are encoded in the quantities $\Delta\alpha(M_Z^2)$ and $\varepsilon_{1,2,3}$ [8]. $\Delta\alpha(M_Z^2)$ originates from the vacuum polarization in the photon propagator caused by the electromagnetic and strong interactions. It is given in terms of known physics below the Z scale, in fact the knowledge of the e^+e^- annihilation cross-section, and amounts to a rather large correction of about 6% [9]. The quantities ε are genuine electroweak corrections which are sensitive to the top quark and the Higgs masses. More generally, any new physics beyond the Standard Model will give contributions to them. Staying within the Standard Model, one gets, for example

$$
\varepsilon_1 = \frac{3G_\mu M_Z^2}{8\pi^2\sqrt{2}}\left\{\left(\frac{m_t^2}{M_Z^2} - 1\right) - 2s_M^2 \ln(M_H/M_Z)\right\} \tag{17}
$$

2.3. A proof of principle: indirect determination of the top quark mass

One of the most striking result from the LEP experiments has been a determination of the top quark mass. In the early period of LEP experimentation, the top quark was still undiscovered because no accelerator had enough energy to produce it, including LEP. Despite this, high-precision measurements of electroweak couplings and of the Z mass provided through Eqs. (16) and (17) a determination of the top quark mass m_t,

$$
m_t^{\text{indirect}} = (172 \pm 14 \pm 19)\ \text{GeV/c}^2 \tag{18}
$$

where the second uncertainty corresponds to an assumed Higgs mass of between 0 and 1 TeV.

The top quark was shortly after discovered in $p\overline{p}$ collisions at FNAL [10], where the highest energy accelerator was operated. The value found for its mass,

$$
m_t^{\text{direct}} = (176 \pm 16)\ \text{GeV/c}^2 \tag{19}
$$

agreed beautifully with the indirect determination from LEP! This result counts as one of the most spectacular findings of the LEP programme, and provides a test of the Standard Model at the level of its quantum corrections. Thus it is a remarkable achievement of particle physics experiment and theory.

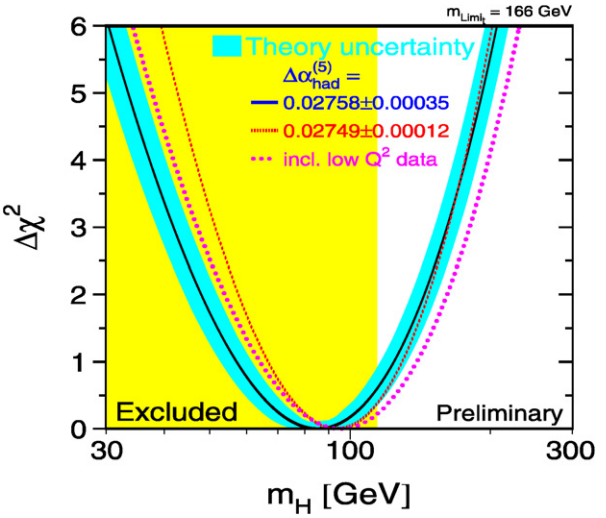

Fig. 3. The global fit of the electroweak observables to the Standard Model predictions provides information on the Higgs boson mass. The figure shows the χ^2 of the fit which reaches a minimum (best description of the measured values by the theory for Higgs masses near 100 GeV/c^2). The blue band gives the uncertainty from the theory calculations, while the yellow region is ruled out by the direct Higgs searches with LEP.

The knowledge of the top quark mass has been since constantly improving, thanks to the FNAL experiments which are still running [11]. The uncertainty will be reduced further at LHC. The current comparison, obtained with a simultaneous determination of the Higgs mass at LEP (see below), yields

$$m_t^{\text{indirect}} = (173 \pm 12)\ \text{GeV/c}^2 \tag{20}$$

$$m_t^{\text{direct}} = (171.4 \pm 2.1)\ \text{GeV/c}^2 \tag{21}$$

2.4. *Sensitivity to the Higgs boson mass*

Once the top quark mass is known from direct measurements, it is easy to see from Eq. (17) that the next most important term in the ϵ_1 correction involves the Higgs boson mass. Since its contribution is only logarithmic in the ratio M_H/M_Z, one does not expect to extract a precise value. However, this is unique information on the Higgs boson, prior to its experimental discovery.

The final LEP result is given in Fig. 3, showing the χ^2 distribution of the global fit of all electroweak observables as function of the Standard Model prediction, dependent on the Higgs mass. The χ^2 minimum yields the most probable value for M_H,

$$M_H = \left(85^{+39}_{-28}\right)\ \text{GeV/c}^2 \tag{22}$$

Despite its poor precision, the result (22) is very important. First, it shows that the Higgs boson mass, which is not fixed by other known parameters of the Standard Model, can be indirectly deduced from quantum loop effects. Then, its mass is found to be relatively light, of the order of 100 GeV/c^2, comparable to the mass of the W and Z vector bosons. This is interesting, because it has been known for some time that perturbative calculations in the Standard Model would fail for Higgs masses in excess of 1 TeV/c^2, as the Higgs boson would behave as a strongly interacting particle in this range. So a light Higgs is good news in this respect! Finally, such a mass range was at least partially accessible for direct production of the Higgs boson at LEP, providing an impetus to run LEP at the highest possible energy.

3. Direct searches for the Higgs boson

Because of its large and unambiguously known coupling to the Z, direct searches for the standard model Higgs boson became the monopoly of LEP. Their results drastically modified the experimental knowledge in the field, even if no discovery took place in the mass region up to 115 GeV/c^2. They remained without competition for a least eight

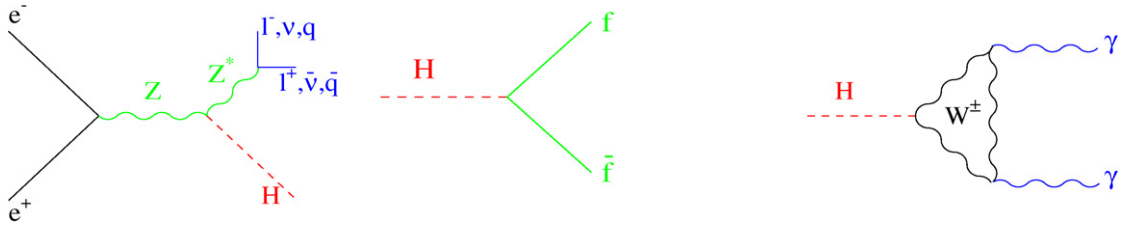

Fig. 4. Feynman diagrams for the Standard Model Higgs boson production at LEP 1 (left), the standard model Higgs boson decay into a pair of fermions (middle) and into a pair of photons (right).

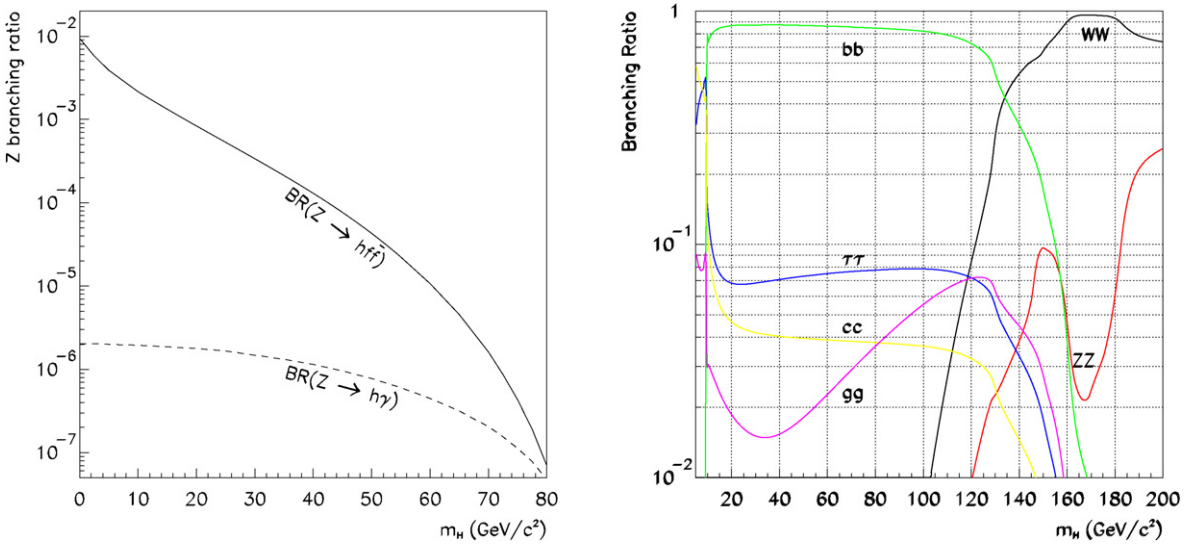

Fig. 5. (Left) Branching ratio of the Z decay into $Hf\bar{f}$ (left axis); (Right) Decay branching fractions of the Higgs boson as a function of its mass (the very low mass region is not represented).

years, still waiting for the Tevatron at FNAL or the LHC at CERN to accumulate sufficient luminosity to become sensitive to a heavier Higgs boson.

3.1. Results from LEP 1

The operation of LEP at and around the Z resonance between 1989 and 1995 (LEP 1) allowed the four detectors to collect a total of about 20 million Z decays. The dominant Z decay leading to Higgs boson production at LEP 1 is called the Higgs-strahlung process, $Z \to Hf\bar{f}$ where f is a neutrino, a charged lepton or a quark, and is sketched in the diagram of Fig. 4. The corresponding Z branching fraction is displayed in Fig. 5 (left) as a function of the Higgs boson mass. With the achieved statistics in the LEP 1 sample, over 10 000 to 100 000 events were expected to be produced for a very light Higgs boson down to about 20 events for a 70 GeV/c^2 Higgs boson.

Beside the production rate, the decay modes of the Z and the Higgs boson (Fig. 4) determine the final state topologies and therefore the search strategy. Because the Higgs boson is expected to couple to the particles proportionally to their mass, it tends to preferentially decay into the pair of heaviest particles kinematically accessible. In Fig. 5, the decay branching fractions of the Higgs boson are shown as a function of its mass. Above the $b\bar{b}$ threshold and in the region of interest at LEP, the Higgs boson mostly decays into $b\bar{b}$, in 85% of the cases. Below this threshold, the Higgs boson may decay into $c\bar{c}$, $\tau^+\tau^-$, $\mu^+\mu^-$, e^+e^-, or into a gluon or a photon pair, leading to a variety of final states with a lower multiplicity than for higher masses.

The high production rate of a light Higgs boson renders the search very easy at LEP 1. As sketched in Fig. 6, three topologies were mainly looked for: (i) acoplanar lepton pairs $\ell^+\ell^-$ from the Z decay, recoiling against missing energy and momentum, to investigate the case in which the Higgs boson is so light (around or below $2m_e$) that its

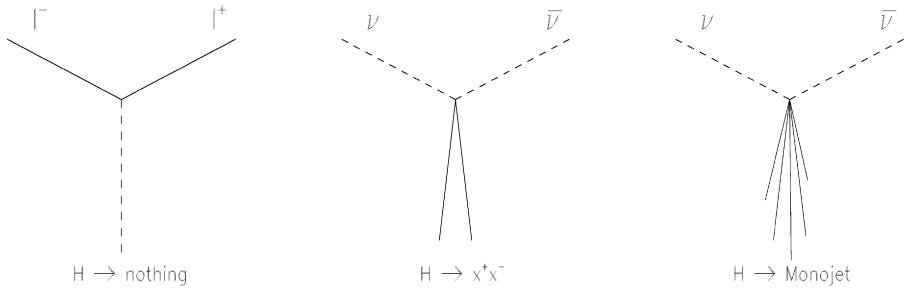

Fig. 6. Final state topologies for the search for a light standard model Higgs boson: acoplanar lepton pair with an invisible Higgs boson (left); acoplanar charged particle pair (middle); and monojet (right).

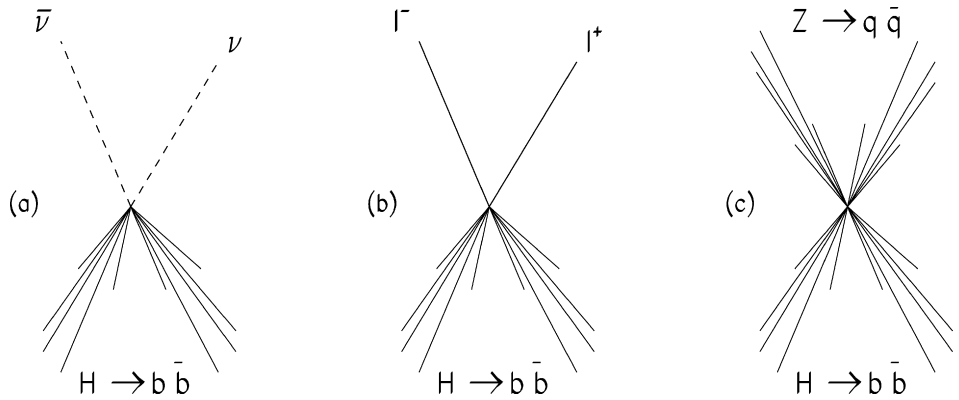

Fig. 7. The acoplanar jets (a) and the energetic lepton pair (b) topologies, are searched for when $M_H \gtrsim 20$ GeV/c^2. The four-jet topology (c) is overwhelmed by background at LEP 1.

lifetime makes it undetectable; (ii) acoplanar pairs of charged particles x^+x^-, recoiling against missing energy and momentum due to $Z^* \to \nu\bar{\nu}$, to deal with the $H \to e^+e^-, \mu^+\mu^-, \tau^+\tau^-, \pi^+\pi^-, \ldots$ decays (for m_{H} between $2m_{\mathrm{e}}$ and 1 GeV/c^2); and (iii) low-multiplicity monojets, recoiling against missing energy and momentum due to $Z^* \to \nu\bar{\nu}$, to take care of the Higgs boson hadronic decays (for M_H up to 20 GeV/c^2). The absence of signal observed in these essentially background-free topologies allowed any Higgs boson mass below $\sim$20 GeV/c^2, including the case in which it is exactly zero, to be excluded at much more than 95% C.L.

For higher Higgs boson masses, the expected final states are different and are mainly made of a Z recoiling against an acoplanar pair of hadronic jets from the Higgs boson decay. Most of these final states are purely hadronic when $Z^* \to q\bar{q}$, and are overwhelmed with the huge background from hadronic Z decays. Only 24% of the final states, leading to the well identifiable topologies displayed in Fig. 7, were therefore used in the search for the Higgs boson by the four experiments: (i) the $(H \to \text{hadrons})(Z^* \to \nu\bar{\nu})$ final state, with two acoplanar jets accompanied with missing energy, called the h$\nu\bar{\nu}$ channel; and (ii) the $(H \to \text{hadrons})(Z^* \to \ell^+\ell^-)$ final state, with $\ell = e$ or μ, with two energetic leptons isolated from the accompanying hadronic system, called the $H\ell^+\ell^-$ channel.

This left only ten (three) events produced for $m_{\mathrm{H}} = 65(70)$ GeV/c^2, to be found within 13 million hadronic Z decays, rendering quite sophisticated the analysis techniques developed for this search [12]. In total, four events were observed in the $H\nu\bar{\nu}$ topology and nine events in the $H\ell^+\ell^-$ topology, well compatible with the 6.0 and 14.6 events expected from standard background processes, mainly from $e^+e^- \to b\bar{b}$ in the $H\nu\bar{\nu}$ channel, and from four-fermion process $e^+e^- \to \ell^+\ell^- q\bar{q}$ in the $H\ell^+\ell^-$ topology.

This agreement between the observation and the standard model expectation allowed each of the four experiments to extract lower limits on the Higgs boson mass: 55.4 (DELPHI), 59.6 (OPAL), 60.2 (L3) and 63.9 GeV/c^2 (ALEPH). In 1995, a combined 95% C.L. lower limit of 65.6 GeV/c^2 was obtained for the Standard Model Higgs boson mass [12].

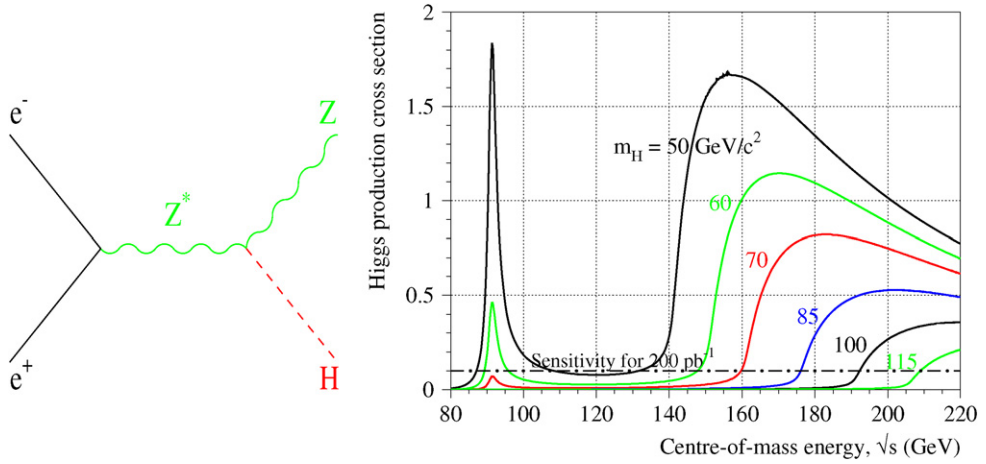

Fig. 8. Higgs boson production process at LEP 2 (left) and cross-section as a function of the centre-of-mass energy for several Higgs boson mass values (right). Also indicated (dash-dotted line) is the 5σ-sensitivity reached with an integrated luminosity of 200 pb^{-1}.

3.2. Results from LEP 2

To go beyond this result, the only efficient solution was to increase the LEP energy above the HZ threshold, $\sqrt{s} > M_H + M_Z$, so as to produce a Z on mass shell and a Higgs boson via the Higgs-strahlung process (Fig. 8). As shown in Fig. 8, a centre-of-mass energy in excess of 160 GeV is required to become sensitive to a 70 GeV/c^2 Higgs boson, and $\sqrt{s} = 192$ GeV is needed to reach $M_H = 100$ GeV/c^2.

For this reason, a total of 288 Nb/Cu superconducting cavities were progressively installed in the LEP tunnel between 1995 and 1999. The design accelerating gradient of 6 MV/m was aimed at compensating the energy lost by e^+'s and e^-'s at $\sqrt{s} = 192$ GeV i.e., which was about 3 GeV per turn. It is worth noting that up to 84 additional cavities could have been installed in the LEP tunnel, which would have allowed a large integrated luminosity to be produced at centre-of-mass energies in excess of 220 GeV.

Although no additional accelerating hardware had been foreseen in 1999 and 2000, the sensitivity continued to increase significantly, from about 100 to 115 GeV/c^2, thanks to the large integrated luminosity produced up to $\sqrt{s} =$ 209.2 GeV. Such high centre-of-mass energies would not have been reached if it were not for the great ingenuity and utmost efforts to take advantage of all possible resources of the collider, with an increase of the accelerating gradient from 6 to 7.5 MV/m.

3.3. A hint at 115 GeV/c^2

The three final state topologies (leptons, acoplanar jets with missing energy, or four jets) arising from HZ production with a Higgs decay in $b\bar{b}$ and Z decays into $\ell^+\ell^-$, $\nu\bar{\nu}$ or $q\bar{q}$, as displayed in Fig. 7, were simultaneously searched for at LEP 2. Unlike at LEP 1, the fully-hadronic final state does not suffer from the huge background from hadronic Z decays. Moreover, the final state Z boson, produced on-shell at LEP 2, provides an additional kinematic constraint, which allows the Higgs boson mass to be reconstructed for each event with a good accuracy, thus further reducing the background from $q\bar{q}$, W^+W^- or ZZ production. Because of its dominant rate ($\sim$70%), the search in the four-jet channel was even found to have a sensitivity to the Higgs boson higher than that of the combination of the missing energy and the leptonic final states.

These clear signatures were selected with efficiencies ranging from 40% for the four-jet final state to 80% for the leptonic case. However clear, these signatures have contributions from the aforementioned standard model background processes, some of which are hardly distinguishable from signal events. To fully take advantage of the topological, kinematical or b-quark content event characteristics allowing signal to be discriminated from backgrounds, likelihood methods or neural networks were used to construct a single combined variable x reflecting the 'signal-ness' of an event. The distributions of this combined variable were used to assess, with large simulated event samples of signal and background, an M_H-dependent signal-to-noise ratio $s(x)/b(x)$, and thus a weight $w(x, M_H) = 1 + s(x)/b(x)$, to

each candidate event. The comprehensive negative log-likelihood $\mathcal{L}(M_H)$ resulting from the product of the weights of the N selected candidate events

$$\mathcal{L}(M_H) = -2\ln Q \quad \text{with } Q = \prod_{i=1}^{N}\left[1 + w_i(x_i, M_H)\right]$$

accounts not only for the number of events observed compared to those expected in the signal and background-only hypotheses, but also for the distribution of the combined variable in the selected data sample.

This log-likelihood is expected to be smaller in the presence of signal than with background events only, and a possible minimum would point to the most likely value for the Higgs boson mass. However, because the signal cross-section decreases rapidly when M_H increases, the separation between a signal-like and a background-only experiment is expected to vanish as M_H reaches the HZ kinematic threshold, $M_H \sim \sqrt{s} - M_Z$. With the 200 pb^{-1} collected by each of the four experiments in the year 2000, their combined likelihood was expected to be sensitive to a signal cross-section of 40 fb, corresponding to eight (less than four) signal events produced in (detected by) each experiment.

Because, until June 2000, no noticeable excess of signal-like candidate events had been seen in the LEP data [13], the whole M_H range below 114.1 GeV/c^2 could be excluded. In June 2000, sizeable luminosity at centre-of-mass energies above 206 GeV (i.e., above the kinematic threshold for a Higgs boson of 115 GeV/c^2) started to be steadily delivered. From this moment onwards, signal-like events compatible with the production of a Higgs boson with mass 115 GeV/c^2 were regularly recorded by the LEP experiments.

In 2001, the data were fully reprocessed and some analyses were re-optimized with numerous systematic studies [13]. The final analysis led to a conservative evaluation of the significance of the excess to 2.1σ [14]. The excess is in agreement with the production of a Higgs boson with mass (115.6 ± 1) GeV/c^2.

The experiments requested an extension of six months of LEP operation in 2001, i.e., with an integrated luminosity of 200 pb^{-1} and an upgraded centre-of-mass energy above 208.5 GeV (made possible with a few available additional cavities and few accelerator tricks). In these conditions the excess could have turned into an unambiguous 5σ discovery, if the effect was genuine and not a statistical fluctuation of the background. Such an extension was not granted by the CERN management, and LEP was shut down for ever on November 17, 2000. This dramatic action brought to a close a decade of extensive, precise, and complete tests of the Standard Model, except for the Higgs boson search, left hanging in the most frustrating situation.

4. Conclusions

The description of electromagnetic and weak phenomena by the $SU(2)_L \times U(1)$ gauge theory has been validated by the measurements of the LEP experiments which tested with high precision the gauge structure of the Standard Model. The generation of the weak boson masses is achieved by spontaneous breaking of the gauge symmetry—the Higgs mechanism—through the introduction of spin-0 fields, out of which only one survives as an observable particle, the famous Higgs boson.

The Higgs mechanism has been indirectly tested through higher-order processes (radiative corrections). The validity of this approach has been established in a spectacular way by deriving successfully the mass of the top quark before its experimental discovery. Precision measurements of couplings and masses:

(1) support the assumption that Higgs fields form weak-isospin doublets, as the value of the ρ parameter at lowest-order is consistent with one; and
(2) provide a determination of the Higgs boson mass, $M_H = (85^{+39}_{-28})$ GeV/c^2, with limited precision due to the logarithmic dependence of the observables on M_H. Such a relatively low-mass restriction, out of a possibly ten times larger range allowed in the perturbative Standard Model, is a major finding of the confrontation between experiment and theory. It is also considered as an indication towards a supersymmetric extension of the Standard Model.

The LEP machine and experiments proved to be extremely efficient in the direct search of the Higgs boson, either on the Z resonance and in the highest energy range near 200 GeV in the centre-of-mass. For the almost complete mass range covered, the Higgs boson has been unambiguously ruled out within the framework of the Standard Model and even of its supersymmetric extensions where more than one Higgs bosons are expected. Pushing LEP to the

frontier energy of 209 GeV gave an indication for a Higgs boson signal near a mass of 115 GeV/c^2, however without enough significance for a discovery to be claimed. The premature stop of the LEP machine in 2000 ended a decade of very successful investigations of the electroweak interactions, but did not allow the confirmation of this signal. Thus the existence of the Higgs boson—the last important experimental confirmation of the Standard Model—is still not established. The hunt for the Higgs in this mass region and higher will resume at the Tevatron and the LHC when they have accumulated enough luminosity.

Acknowledgements

I wish to thank Fawzi Boudjema and Patrick Janot for allowing me to make an extensive use of their excellent reviews [15,16] in the special issue of the Comptes Rendus "Advances in Particle Physics: the LEP Contribution" I had the pleasure to coordinate in 2002.

References

[1] S.L. Glashow, Nucl. Phys. 22 (1961) 579;
S. Weinberg, Phys. Rev. Lett. 19 (1967) 1264;
A. Salam, in: N. Svartholm (Ed.), Proc. 8th Nobel Symposium, Almqvist and Wiksells, Stockholm, 1968, p. 367.
[2] P.W. Higgs, Phys. Lett. 12 (1964) 132;
P.W. Higgs, Phys. Rev. 145 (1966) 1156;
T.W. Kibble, Phys. Rev. 155 (1967) 1554;
See also J. Goldstone, A. Salam, S. Weinberg, Phys. Rev. 127 (1962) 965;
F. Englert, R. Brout, Phys. Rev. Lett. 13 (1964) 321.
[3] N. Cabibbo, Phys. Rev. Lett. 10 (1963) 531;
M. Kobayashi, K. Maskawa, Prog. Theor. Phys. 49 (1973) 652.
[4] S.L. Glashow, J.I. Illiopoulos, L. Maiani, Phys. Rev. D 2 (1970) 1285.
[5] The LEP/SLD Collaborations and Electroweak Working Groups, hep-ex/0509008, Phys. Rep. 427 (2006) 257;
The LEP Collaborations and Electroweak Working Group, hep-ex/0511027;
See also http://lepewwg.web.cern.ch.
[6] G. Gabrielse, et al., Phys. Rev. Lett. 97 (2006) 030802.
[7] G. 't Hooft, M. Veltman, Nucl. Phys. 44 (1972) 189.
[8] G. Altarelli, R. Barbieri, Phys. Lett. B 253 (1991) 161;
For another parametrisation see M.E. Peskin, T. Takeuchi, Phys. Rev. D 46 (1992) 381.
[9] See for instance M. Davier, A. Höcker, Phys. Lett. B 419 (1998) 419.
[10] CDF Collaboration, F. Abe, et al., Phys. Rev. Lett. 74 (1995) 2626;
D0 Collaboration, Phys. Rev. Lett. 74 (1995) 2632.
[11] The Tevatron Electroweak Working Group for the CDF and D0 Collaboration, hep-ex/0608032.
[12] ALEPH Collaboration, D. Buskulic, et al., Phys. Lett. B 384 (1996) 427;
OPAL Collaboration, G. Alexander, et al., Z. Phys. C 73 (1997) 189;
L3 Collaboration, M. Acciarri, et al., Phys. Lett. B 385 (1996) 454;
DELPHI Collaboration, P. Abreu, et al., Nucl. Phys. B 421 (1994) 3;
P. Janot, Nucl. Phys. B (Proc. Suppl.) 38 (1995) 264.
[13] ALEPH Collaboration, A. Heister, et al., Phys. Lett. B 526 (2002) 191;
DELPHI Collaboration, P. Abreu, et al., Phys. Lett. B 499 (2001) 23;
L3 Collaboration, M. Acciari, et al., Phys. Lett. B 495 (2000) 18;
L3 Collaboration, P. Achard, et al., Phys. Lett. B 517 (2001) 319;
OPAL Collaboration, G. Abbiendi, et al., Phys. Lett. B 499 (2001) 38.
[14] The LEP Higgs working group, CERN-EP/2001-055 (2001).
[15] F. Boudjema, D. Zeppenfeld, C. R. Physique 3 (2002) 1097.
[16] P. Janot, M. Kado, C. R. Physique 3 (2002) 1193.